

# Quantum interference controls the electron spin dynamics in $n$ -GaAs

V. V. Belykh,<sup>1,2,\*</sup> A. Yu. Kuntsevich,<sup>2</sup> M. M. Glazov,<sup>3,4,†</sup> K. V. Kavokin,<sup>3,4</sup> D. R. Yakovlev,<sup>1,3</sup> and M. Bayer<sup>1,3</sup>

<sup>1</sup>*Experimentelle Physik 2, Technische Universität Dortmund, D-44221 Dortmund, Germany*

<sup>2</sup>*P.N. Lebedev Physical Institute of the Russian Academy of Sciences, 119991 Moscow, Russia*

<sup>3</sup>*Ioffe Institute, Russian Academy of Sciences, 194021 St. Petersburg, Russia*

<sup>4</sup>*Spin Optics Laboratory, St. Petersburg State University, 199034 St. Petersburg, Russia*

(Dated: December 3, 2024)

Manifestations of quantum interference effects in macroscopic objects are rare. *Weak localization* is one of the few examples of such effects showing up in the electron transport through solid state. Here we show that weak localization becomes prominent also in optical spectroscopy via detection of the electron spin dynamics. In particular, we find that weak localization controls the free electron spin relaxation in semiconductors at low temperatures and weak magnetic fields by slowing it down by almost a factor of two in  $n$ -doped GaAs in the metallic phase. The weak localization effect on the spin relaxation is suppressed by moderate magnetic fields of  $\sim 1$  T which destroy the interference of electron trajectories and by increasing the temperature. The weak localization suppression causes an anomalous decrease of the longitudinal electron spin relaxation time  $T_1$  with magnetic field, in stark contrast with well-known magnetic field induced increase in  $T_1$ . This is consistent with transport measurements which show the same variation of resistivity with magnetic field. Our discovery opens a vast playground to explore quantum magneto-transport effects optically in the spin dynamics.

The design of future spintronic and opto-spintronic devices requires a detailed understanding of the correlation between the electron conductivity and spin relaxation in prospective material systems, such as semiconductors. The electron spin relaxation in semiconductors depends strongly on whether electrons are itinerant or localized [1, 2]. Across the metal-to-insulator transition (MIT) the spin relaxation changes as dramatically as does the conductivity [2, 3]. Indeed, in the insulating phase both conductivity and spin relaxation critically depend on the overlap of the wavefunctions of donor-bound electrons at low temperatures and on the number of delocalized electrons at higher temperatures. In the metallic phase, in semiconductors without an inversion center with GaAs as prototype system, the spin relaxation is governed by spin-orbit coupling [4] and, similarly to the conductivity, the spin polarization becomes suppressed by electron scattering events. The spin relaxation rate is closely related to the electron diffusion coefficient [5–7], so that charge transport phenomena are generally expected to manifest also in spin relaxation processes [8–10]. The situation becomes particularly involved in the vicinity of the MIT where quantum effects become important [11, 12].

While the mechanisms of electron spin relaxation in semiconductors were largely clarified in theory back in the 1970s [13], for a long time experiments could access the electron spin dynamics only via the Hanle effect near zero magnetic field. Since the 1990s more advanced techniques have become available such as pump-probe methods analyzing the Kerr/Faraday rotation [14, 15] or polarization-resolved photoluminescence [16–19], and elaborated methods like resonant spin amplification [20, 21], spin noise spectroscopy [22–24] and spin inertia reorientation [25]. Each of these tools has limita-

tions related to the achievable time resolution, the addressable time range or the applicable magnetic field. So far, access to the relation between the electron diffusion and spin relaxation in the vicinity of the MIT was hindered by experimental limitations. Only recently the pump-probe technique was extended to facilitate direct measurements of arbitrarily long spin dynamics with picosecond time resolution across a wide range of magnetic fields [26].

On the other hand, the transport properties of semiconductors that directly provide information about electron diffusion, are rather easily accessible in experiment. In weak magnetic fields the low temperatures magnetoresistance is negative due to the weak localization effect: the magnetic field destroys the phase coherence of interfering paths and increases the electron diffusion coefficient [27–34]. The spin-orbit interaction has a pronounced impact on the low field magnetoresistance leading to positive magnetoresistance, i.e., antilocalization, if the electron spin coherence is lost faster than its phase [27]. Although weak localization/antilocalization is expected to emerge in the spin dynamics [12, 35], it has not been identified in experiments so far.

In this paper we demonstrate that weak localization significantly slows down the itinerant electron spin relaxation in the Dyakonov-Perel' mechanism. Using the extended pump-probe Faraday rotation technique we study the longitudinal electron spin relaxation time  $T_1$  as a function of external magnetic field in  $n$ -doped metallic bulk GaAs. While the classical theory [36] predicts an increase of  $T_1$  with increasing field, we observe an anomalous decrease of  $T_1$  in moderate fields  $B \lesssim 1$  T. From transport measurements done on the same samples we observe that the negative magnetoresistance is correlated with the anomalous magnetic field dependence of

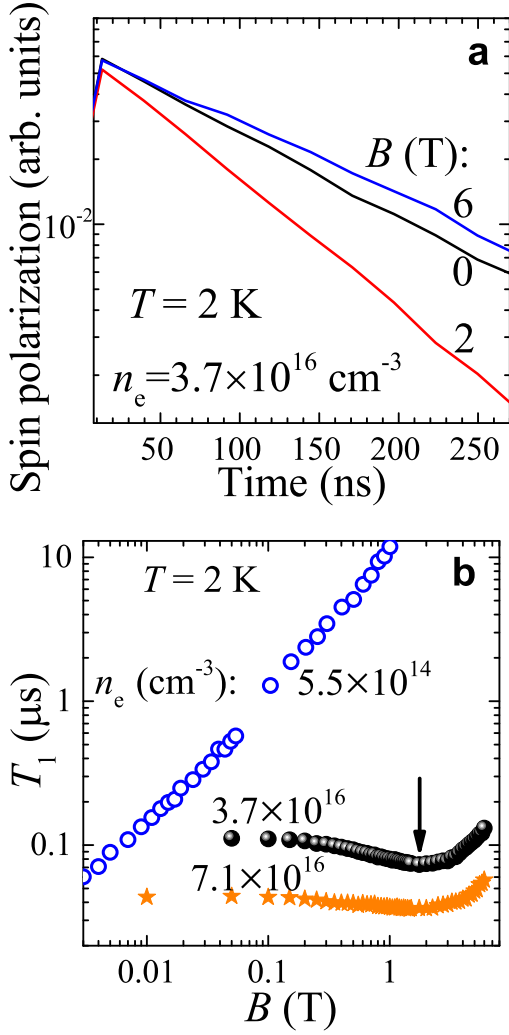


FIG. 1. Longitudinal electron spin relaxation. **a** Dynamics of the electron spin polarization (measured as Faraday rotation signal) at different magnetic fields for the  $n$ -GaAs sample with  $n_e = 3.7 \times 10^{16} \text{ cm}^{-3}$ . **b** Magnetic field dependence of the longitudinal relaxation time  $T_1$  for samples with different donor concentrations. The arrow indicates the minimum in the  $T_1(B)$  dependence. **a,b**  $T = 2 \text{ K}$ .

$T_1$ . We develop a theoretical model of the weak localization effect in the spin relaxation of bulk semiconductors and find very good agreement between the calculations and experimental data. Our results establish a strict relation between the electron diffusion and spin relaxation in metallic systems in the vicinity of the MIT. Thereby all-optical access to weak localization is provided and a tool to probe *locally* electron transport phenomena is developed.

## RESULTS

*Experiment.* The circularly polarized pump laser pulse creates spin polarization along the magnetic field (Faraday geometry  $\mathbf{B} \parallel z \parallel [001]$ ) which can be detected by the delayed probe laser pulse via Faraday rotation of its linear polarization. Figure 1a shows the dynamics of the spin polarization for exemplary values of the external magnetic field  $B = 0, 2$  and  $6 \text{ T}$  for the metallic sample with electron concentration  $n_e = 3.7 \times 10^{16} \text{ cm}^{-3}$ , which is somewhat above the MIT threshold,  $n_e^{\text{MIT}} \approx (1-2) \times 10^{16} \text{ cm}^{-3}$ . The signal decays monoexponentially with the longitudinal spin relaxation time  $T_1$ . It is seen from Fig. 1a that as the magnetic field grows,  $T_1$  first decreases, reaches a minimum and then increases. The non-monotonic dependence of  $T_1(B)$  with a minimum at about  $1.5 \text{ T}$  is further substantiated in Fig. 1b by the solid spheres. The minimum in the  $T_1(B)$  dependence is observed for the sample with even higher carrier concentration becoming less pronounced, while for the samples with lower donor concentrations, below MIT,  $T_1$  monotonically increases with increasing  $B$  (the open circles in Fig. 1b).

To investigate the anomalous  $T_1(B)$  dependence further we perform measurements at different temperatures with the results summarized in Fig. 2a. Interestingly, the minimum in the  $T_1(B)$  dependence is observed only at low temperatures  $T \lesssim 14 \text{ K}$ . Furthermore, with increasing temperature the minimum becomes less pronounced due to the decrease of the zero-field  $T_1$  value. The decrease of  $T_1$  with magnetic field or temperature increase are unexpected in view of existing theories of free-electron spin relaxation in semiconductors [4, 7, 36]. This calls for a detailed modeling of the spin relaxation process which is presented below.

*Model.* In GaAs-like semiconductors, being in the metallic phase, the spin relaxation is controlled by the Dyakonov-Perel mechanism [13]: the electron spin precesses around the effective, spin-orbit coupling-induced magnetic field and the spin precession is randomized by scattering events. The spin dynamics is described in the framework of a kinetic equation for the spin distribution function  $\mathbf{s}_k$  [4, 7, 36–38]

$$\frac{\partial \mathbf{s}_k}{\partial t} + \mathbf{s}_k \times \boldsymbol{\Omega}_k + \boldsymbol{\Lambda}_k \{ \mathbf{s}_k \} = Q \{ \mathbf{s}_k \}. \quad (1)$$

Here  $\boldsymbol{\Omega}_k$  is spin precession frequency proportional to the cube of the electron wavevector  $\mathbf{k}$  in a term related with the bulk inversion asymmetry, the operator  $\boldsymbol{\Lambda}_k = -\omega_c [\mathbf{k} \times \partial / \partial \mathbf{k}]$  describes the electron cyclotron motion in the external magnetic field,  $\omega_c = e\mathbf{B}/mc$  is the cyclotron frequency,  $m$  is the electron effective mass and  $e$  is the electron charge (the Zeeman splitting is neglected). In the last term in Eq. (1),  $Q \{ \mathbf{s}_k \}$  is the collision integral, i.e., the operator describing the redistribution of electrons between different states in  $\mathbf{k}$ -space. It is de-

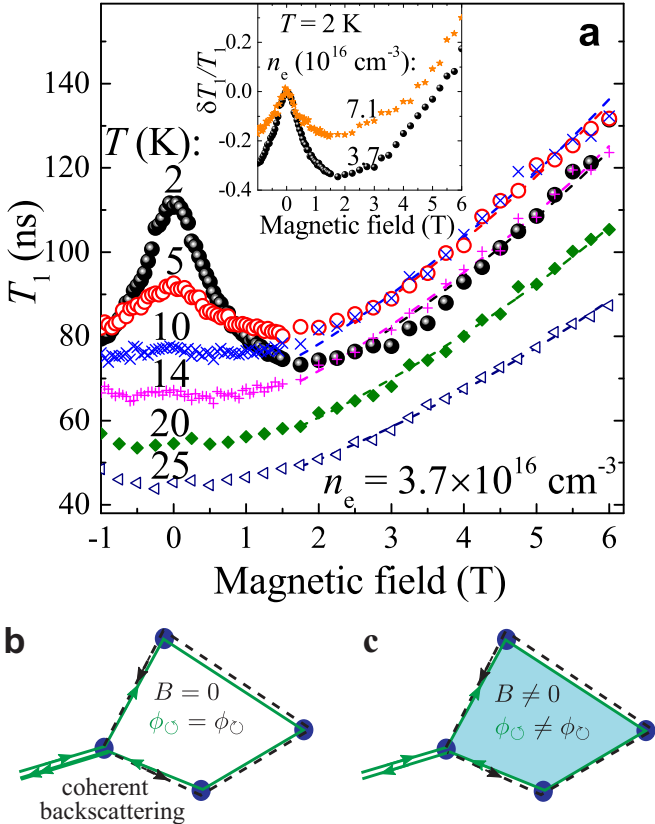


FIG. 2. Effect of weak localization on longitudinal spin relaxation time  $T_1$ . **a** Magnetic field dependence of  $T_1$  at different temperatures.  $n_e = 3.7 \times 10^{16} \text{ cm}^{-3}$ . The dashed lines show fits to the experimental data with Eq. (3). Inset shows relative variation of  $T_1$  with magnetic field for metallic samples with different electron concentrations. **b** Scheme of constructive interference of clockwise and counter-clockwise electrons paths, starting at the same impurity and related by the time reversal symmetry. The interference gives rise to the weak localization effect by increasing the backscattering efficiency. **c** The interference between the same paths as in Fig. 2b is destroyed by the magnetic field due to the extra phase acquired by the electron traveling clockwise and counter-clockwise.

scribed by a set of relaxation times  $\tau_m$  ( $m = 1, 2, 3, \dots$ ) describing the relaxation of different angular harmonics of the distribution function. Note, that  $\tau_1 = \tau_p$  describes the momentum relaxation of electrons. In a classical approach, these relaxation times are independent of the magnetic field.

The longitudinal spin relaxation time for degenerate electrons in bulk GaAs at  $B = 0$  takes the form [4]

$$T_1(0) = \frac{105}{32\alpha^2} \frac{\hbar^2 E_g}{E_F^3 \tau_3}, \quad (2)$$

where  $E_F$  is the electron Fermi energy,  $E_g = 1.52 \text{ eV}$  is the band gap energy and  $\alpha \approx 0.063$  is the dimensionless Dresselhaus constant for GaAs, recalculated from data in Refs. [39, 40]. The magnetic field dependence of  $T_1$  was

calculated in Ref. [36]:

$$\frac{T_1(B)}{T_1(0)} = \frac{[1 + (\omega_c \tau_3)^2][1 + 9(\omega_c \tau_3)^2]}{1 + 6(\omega_c \tau_3)^2} \approx 1 + 4\omega_c^2 \tau_3^2. \quad (3)$$

This equation shows the spin relaxation suppression by the magnetic field due to the electron performing cyclotron motion. The last approximate equality in Eq. (3) holds for  $\omega_c \tau_3 \ll 1$ . Equation (3) clearly demonstrates an increase in the spin relaxation time  $T_1$  with growing magnetic field. This expression with the temperature-independent  $\tau_3 \approx 40 \text{ fs}$  describes the experimental data at  $B \gtrsim 2 \text{ T}$  (the dashed lines in Fig. 2a). From the value of  $T_1$  extrapolated to  $B = 0$ , we obtain  $\tau_3 \approx 40 \text{ fs}$  after Eq. (2), in good agreement with the value obtained above from the  $B$ -dependence.

The classical theory of Dyakonov-Perel spin relaxation mechanism, expressed by Eqs. (2) and (3), as well as additional possible mechanisms of spin relaxation due to the  $g$ -factor spread [41] cannot, however, explain the sizable decrease of the spin relaxation time  $T_1$  in rather weak magnetic fields  $B \lesssim 1 \text{ T}$  and at low temperatures  $T \lesssim 14 \text{ K}$ . Clearly, other effects, not accounted for by the approach in Refs. [4, 7, 36–38] must play an important role in our experiment. In fact, in the derivation of Eqs. (2) and (3) the electron dynamics is assumed to be classical, i.e., the inequality  $E_F \tau_p / \hbar \gg 1$  is assumed to hold. For relatively low electron densities,  $E_F \tau_p / \hbar$  just slightly exceeds unity and quantum effects start to play a role. In particular, for an electron traveling through a disordered medium the interference between classical trajectories, as schematically depicted in Fig. 2b becomes important. For electron waves traveling clockwise and counter-clockwise through the same configuration of impurities, the phases acquired on these two paths,  $\phi_O = \phi_O = \oint \mathbf{k} dl$ , are the same. As a result, the two paths shown by the solid and dashed lines interfere constructively, leading to coherent backscattering. In effect, the scattering efficiency by the impurities increases and the electron propagation slows down. This is the *weak localization* effect signifying the onset of the MIT with decreasing electron density. Importantly, a magnetic field destroys the constructive interference owing to the extra phase proportional to the field flux through the trajectory acquired by the diffusing electron, see Fig. 2c. Indeed, for clockwise and counter-clockwise propagation the field-induced phases are opposite, hence, the magnetic field suppresses the weak localization [27, 32–34, 42].

In order to account for the interference effect we follow the semiclassical approach where, as illustrated in Fig. 2b,c, the quantum effects are accounted for by renormalization of the cross-section for electron scattering by the impurity [12, 35, 43]. The momentum relaxation time  $\tau_p$  acquires a correction  $\delta\tau_p$  of the form

$$\frac{\delta\tau_p}{\tau_p} = -\frac{2mD}{\pi\hbar n_e} \sum_{s,s'=\pm 1/2} \mathcal{C}_{ss's's}(\mathbf{r} = 0), \quad (4)$$

where  $D = v_F^2 \tau_p / 3$  is the electron diffusion coefficient, and  $v_F$  is the Fermi velocity. In Eq. (4),  $\mathcal{C}_{s_1 s_2 s_3 s_4}(\mathbf{r} = 0)$  is the Cooperon matrix describing the electron interference along the closed loops, which is calculated via a standard diagram technique [27]. Similarly, the interference effects modify the relaxation time of the third angular harmonics of the spin distribution function,  $\tau_3$ , which defines the spin relaxation time [Eq. (2)], as:

$$\frac{\delta\tau_3}{\tau_3} = -\frac{2mD}{\pi\hbar n_e} \sum_{s,s'=\pm 1/2} \mathcal{C}_{ss's's}(\mathbf{r} = 0)(2\delta_{ss'} - 1). \quad (5)$$

The factor  $(2\delta_{ss'} - 1)$  is due to the spin vortices in the corresponding diagrams [12, 35]. We introduce the phase relaxation time  $\tau_\phi$  associated with inelastic electron-electron or electron-phonon scattering processes, and consider hereafter the diffusive regime where  $\tau_\phi \gg \tau_p, \tau_3$  and the magnetic length  $l_B = \sqrt{\hbar c / (|e|B)}$  exceeds by far the mean free path,  $l_B \gg v_F \tau_p$ . Moreover, we impose the condition of rather weak spin orbit interaction,  $T_1(0) \gg \tau_\phi$ , meaning that the electron spin is conserved during passage through the closed loops in which the interference takes place. As a result, we have

$$\frac{\delta T_1(B)}{T_1(0)} = \frac{\delta \rho(B)}{\rho(0)} = -\frac{m}{2\pi^2 \hbar n_e \tau_p} \sqrt{\frac{|e|B}{\hbar c}} F_3 \left( \frac{B_\phi}{4B} \right). \quad (6)$$

Here  $B_\phi = \hbar c / (|e|l_\phi^2)$ ,  $l_\phi = \sqrt{D\tau_\phi}$  is the phase relaxation length, and the function  $F_3(x)$  is defined as

$$F_3(x) = \sum_{n=0}^{\infty} \left[ 2(\sqrt{n+1+x} - \sqrt{n+x}) - \frac{1}{\sqrt{n+1/2+x}} \right].$$

Note that for  $x \ll 1$   $F_3(x) \approx 0.605$  and for  $x \gg 1$ ,  $F_3(x) \approx 1/(48x^{3/2})$ .

*Discussion and comparison of electron spin dynamics and transport.* To independently experimentally confirm the presence of weak localization and estimate its magnitude in the considered system, we have also measured the *magnetoresistance* (see Fig. 3a) on the same samples. The low-field negative magnetoresistance is clearly seen, in agreement with previous works it arises from the weak localization effect [28–34]. At high fields positive magnetoresistance is observed, presumably due to the field-induced compression of electron wave functions on donors and also possibly due to the onset of Shubnikov-de Haas oscillations. The observed behavior is qualitatively similar to that for  $T_1(B)$  (Fig. 2a) and, in particular, the scale of the weak localization magnetic field is the same. Further, the negative magnetoresistance persists in the same range of temperatures as the decrease of  $T_1$  with  $B$ .

Furthermore, according to Eq. (6), the relative change of  $T_1$  and  $\rho$  due to the weak localization should be the same. Figure 3b shows these relative variations of  $T_1$  (the spheres) and  $\rho$  (the solid lines),  $\delta T_1/T_1 \equiv T_1(B)/T_1(0) - 1$

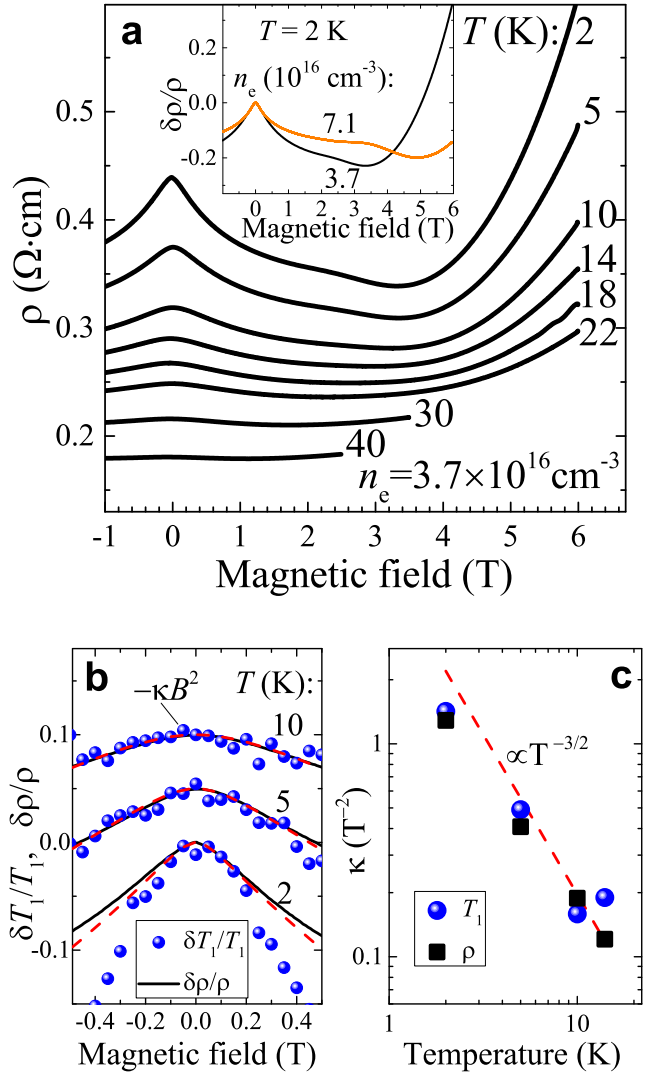


FIG. 3. Evidence of weak localization in resistivity measurements. **a** Magnetic field dependence of the resistivity  $\rho$  at different temperatures. Inset shows relative variation of  $\rho$  with magnetic field for metallic samples with different electron concentrations. **b** Relative variation of  $T_1$  (the symbols) and  $\rho$  (the solid lines) with magnetic field at different temperatures. The red dashed lines show fits to both  $\Delta T_1/T_1$  and  $\delta\rho/\rho$  with Eq. (6). The curves are vertically shifted for clarity. **c** Curvatures of the magnetic field dependencies of  $\delta T_1/T_1$  (the spheres) and  $\delta\rho/\rho$  (the squares),  $\kappa$  in Eq. (7), as a function of temperature. The red dashed line shows a  $T^{-3/2}$  dependence. **a-c**  $n_e = 3.7 \times 10^{16} \text{ cm}^{-3}$ .

and  $\delta\rho/\rho \equiv \rho(B)/\rho(0) - 1$ , with magnetic field, respectively. Equation (6) is, strictly speaking, valid if the quantum corrections are small, i.e. for  $\delta T_1/T_1, \delta\rho/\rho \ll 1$  which is not the case in our sample right above the MIT. Nevertheless, the measured magnetic field dependences of  $\delta T_1/T_1$  and  $\delta\rho/\rho$  are in remarkable agreement in weak magnetic fields. The analysis of the asymptotic form of

Eq. (6) shows that in weak fields  $B \ll B_\phi$

$$\frac{\delta T_1(B)}{T_1(0)} = \frac{\delta \rho(B)}{\rho(0)} = -\kappa B^2, \quad (7)$$

with the prefactor  $\kappa = 0.048(e/mc)^2 \sqrt{\tau_p \tau_\phi^3}$ . In the studied temperature range  $\tau_p$  is constant, as found above, and  $\tau_\phi = A/T$ , where  $A$  is a constant, in accordance with Refs. [34, 44]. Thus,  $\kappa \propto T^{-3/2}$ . The values of curvature  $\kappa$  corresponding to  $T_1$  and  $\rho$  extracted from the fit are shown in 3c. They are in very good agreement and follow a  $T^{-3/2}$  dependence as shown by the red dashed line.

The dashed lines in Fig. 3b show fits to the experiment by Eq. (6) using a reasonable set of parameters, namely  $\tau_p = 55$  fs (temperature independent) and  $\tau_\phi = A/T$  with  $A = 19$  ps·K. Such inverse temperature dependence of the phase relaxation time was observed for a similar GaAs system [34] with  $n_e = 2.9 \times 10^{16}$  cm<sup>-3</sup> giving a similar value of  $A \approx 12$  ps·K. In order to compare the value  $\tau_p = 55$  fs with the previously obtained  $\tau_3 = 40$  fs we calculated the ratio of  $\tau_p/\tau_3$  by angular integration of the cross-section of partial scattering at the screened Coulomb potential of charged impurities. For the parameters of our sample the ratio  $\tau_p/\tau_3 = 1.7$  and does not reach the asymptotic value of 6, obtained for an extremely small scattering angle [4]. Thus, the time  $\tau_3$  obtained by considering classical Dyakonov-Perel relaxation is in good agreement with the time  $\tau_p$  derived from the weak localization anomaly.

We have also studied the magnetic field dependencies of  $T_1$  and  $\rho$  for a sample with higher electron concentration  $n_e = 7.1 \times 10^{16}$  cm<sup>-3</sup>. The corresponding results are presented in the insets in Figs. 2a and 3a. One can see that the effect of weak localization is reduced by a factor of about two for  $n_e = 7.1 \times 10^{16}$  cm<sup>-3</sup> compared to the sample with  $n_e = 3.7 \times 10^{16}$  cm<sup>-3</sup> as expected from Eq. (6) which contains  $n_e$  in the denominator. The times  $\tau_3$ ,  $\tau_p$  and  $\tau_\phi$  are similar for both samples.

## DISCUSSION

We have demonstrated that the weak localization of electrons has pronounced impact on their spin dynamics. The longitudinal spin relaxation time  $T_1$  in  $n$ -doped GaAs, being in the metallic phase, demonstrates an anomalous decrease with increasing magnetic field at low temperatures. This decrease is due to the field-induced destruction of phase coherence for electrons resulting in the suppression of the weak localization. This shows that physics studied in transport experiments capturing the entirety of physical phenomena between the electrical contacts may be studied locally using focused optical probes of the spin dynamics. The potential of this approach will be very prominent also in two-dimensional

systems where one can expect visualization of the weak localization induced non-exponential tails in spin polarization.

## METHODS

The results are obtained on Si-doped GaAs samples with electron concentrations of  $n_e = 5.5 \times 10^{14}$  cm<sup>-3</sup> (2- $\mu$ m-thick layer grown by the molecular-beam epitaxy), as well as  $3.7 \times 10^{16}$  cm<sup>-3</sup> and  $7.1 \times 10^{16}$  cm<sup>-3</sup> (140 and 170- $\mu$ m-thick bulk wafers, respectively).

For optical measurements the samples are placed in the variable temperature insert of a split-coil magnetocryostat ( $T = 2$ –25 K). Magnetic fields up to 6 T are applied parallel to the light propagation direction that is parallel to the sample growth axis (Faraday geometry). The extended pump-probe Kerr/Faraday rotation technique is used to study the electron spin dynamics. It is a modification of the standard pump-probe Kerr/Faraday rotation technique, where circularly-polarized pump pulses generate carrier spin polarization, which is then probed by the Kerr(Faraday) rotation of linearly-polarized probe pulses after reflection(transmission) from(through) the sample. Implementation of pulse picking for both pump and probe beams in combination with a mechanical delay line allows us to scan microsecond time ranges with picosecond time resolution. Details of the technique are given in Ref. [26].

Here, a Ti:Sapphire laser emits a train of 2 ps pulses with a repetition rate of 76 MHz (repetition period  $T_R = 13.1$  ns). The pump protocol uses single pulse per excitation period. The separation between these pulses is  $80T_R$ ,  $160T_R$  or  $320T_R$  in order to clearly exceed the characteristic time of spin polarization decay. The sample with donor concentration  $n_e$  of  $5.5 \times 10^{14}$  cm<sup>-3</sup> is studied in reflection geometry (Kerr rotation) with the laser wavelength set to 819 nm, close to the donor-bound exciton resonance. The samples with  $n_e = 3.7 \times 10^{16}$  cm<sup>-3</sup> and  $7.1 \times 10^{16}$  cm<sup>-3</sup> are studied in transmission geometry (Faraday rotation) with the laser wavelength set to 829 nm.

Magnetoresistance measurements were performed using a standard 4-terminal technique with a lock-in amplifier. The measurement current (36 Hz, 100  $\mu$ A) was checked not to overheat the sample at the lowest temperature. Ohmic contacts (with an almost  $T$ -independent resistance of about 100 Ohm) were obtained by annealing of indium drops on top of the preliminary scratched wafer (10 minutes at 400°C in vacuum). A PPMS-9 cryostat and Cryogenics CFMS-16 system were used to set the temperature (2–40 K) and magnetic field (up to 6 T). The magnetic field perpendicular to the sample surface and current direction was swept from positive to negative values with subsequent symmetrization of the data to compensate inevitable contact misalignment.

## ACKNOWLEDGMENTS

We are grateful to S. A. Crooker for providing the samples, and to A. Greilich, and E. Evers for valuable advice and useful discussions. We acknowledge the financial support of the Deutsche Forschungsgemeinschaft in the frame of the ICRC TRR 160 (project A1). MMG was partially supported by the RFBR Project No. 15-52-12012, RF President grant MD-1555.2017.2, and the program of RAS “Nanostructures”. KVK and MMG acknowledge support from Saint-Petersburg State University via a research grant 11.34.2.2012. Magnetotransport measurements have been performed using research equipment of the LPI Shared Facility Center.

\* [vasilii.belykh@tu-dortmund.de](mailto:vasilii.belykh@tu-dortmund.de)

† [glazov@coherent.ioffe.ru](mailto:glazov@coherent.ioffe.ru)

- [1] Dzhioev, R. I. *et al.* Low-temperature spin relaxation in n-type GaAs. *Phys. Rev. B* **66**, 245204 (2002).
- [2] Belykh, V. V., Kavokin, K. V., Yakovlev, D. R. & Bayer, M. Electron charge and spin delocalization revealed in the optically probed longitudinal and transverse spin dynamics in n-GaAs. *Phys. Rev. B* **96**, 241201 (2017).
- [3] Lonnemann, J. G., Rugeramigabo, E. P., Oestreich, M. & Hübner, J. Closing the gap between spatial and spin dynamics of electrons at the metal-to-insulator transition. *Phys. Rev. B* **96**, 045201 (2017).
- [4] Dyakonov, M. I. & Perel, V. I. Spin relaxation of conduction electrons in noncentrosymmetric semiconductors. *Fiz. Tverd. Tela* **13**, 3581 (1972) [Sov. Phys. Solid State 13, 3023 (1972)].
- [5] Kavokin, K. V. Spin relaxation of localized electrons in n-type semiconductors. *Semicond. Sci. Technol.* **23**, 114009 (2008).
- [6] Dyakonov, M. & Kachorovskii, V. Spin relaxation of two-dimensional electrons in noncentrosymmetric semiconductors. *Sov. Phys. Semicond.* **20**, 110 (1986).
- [7] Dyakonov, M. I. (ed.) *Spin Physics in Semiconductors*, vol. 157 of *Springer Series in Solid-State Sciences* (Springer International Publishing, Cham, 2017).
- [8] Sih, V. *et al.* Control of electron-spin coherence using Landau level quantization in a two-dimensional electron gas. *Phys. Rev. B* **70**, 161313 (2004).
- [9] Larionov, A. V., Kulik, L. V., Dickmann, S. & Kukushkin, I. V. Goldstone mode stochasticization in a quantum Hall ferromagnet. *Phys. Rev. B* **92**, 165417 (2015).
- [10] Larionov, A. V., Stepanets-Khussein, E. & Kulik, L. V. Spin dephasing of a two-dimensional electron gas in a GaAs quantum well near odd filling factors. *JETP Lett.* **105**, 238–240 (2017).
- [11] Shklovskii, B. I. Dyakonov-Perel spin relaxation near the metal-insulator transition and in hopping transport. *Phys. Rev. B* **73**, 193201 (2006).
- [12] Lyubinskiy, I. S. & Kachorovskii, V. Y. Slowing down of spin relaxation in two-dimensional systems by quantum interference effects. *Phys. Rev. B* **70**, 205335 (2004).
- [13] Pikus, G. E. & Titkov, A. N. Spin relaxation under optical orientation in semiconductors. In Meier, F. & Zakharchenya, B. P. (eds.) *Opt. Orientat.*, 109 (North-Holland, Amsterdam, 1984).
- [14] Baumberg, J. J., Awschalom, D. D., Samarth, N., Luo, H. & Furdyna, J. K. Spin beats and dynamical magnetization in quantum structures. *Phys. Rev. Lett.* **72**, 717–720 (1994).
- [15] Zheludev, N. *et al.* Giant specular inverse Faraday effect in Cd0.6Mn0.4Te. *Solid State Commun.* **89**, 823–825 (1994).
- [16] Colton, J. S., Kennedy, T. A., Bracker, A. S. & Gammon, D. Microsecond spin-flip times in n-GaAs measured by time-resolved polarization of photoluminescence. *Phys. Rev. B* **69**, 121307 (2004).
- [17] Colton, J. S. *et al.* Anomalous magnetic field dependence of the T1 spin lifetime in a lightly doped GaAs sample. *Phys. Rev. B* **75**, 205201 (2007).
- [18] Fu, K.-M. C. *et al.* Millisecond spin-flip times of donor-bound electrons in GaAs. *Phys. Rev. B* **74**, 121304 (2006).
- [19] Linpeng, X. *et al.* Longitudinal spin relaxation of donor-bound electrons in direct band-gap semiconductors. *Phys. Rev. B* **94**, 125401 (2016).
- [20] Kikkawa, J. M. & Awschalom, D. D. Resonant Spin Amplification in n-Type GaAs. *Phys. Rev. Lett.* **80**, 4313 (1998).
- [21] Yugova, I. A., Glazov, M. M., Yakovlev, D. R., Sokolova, A. A. & Bayer, M. Coherent spin dynamics of electrons and holes in semiconductor quantum wells and quantum dots under periodical optical excitation: Resonant spin amplification versus spin mode locking. *Phys. Rev. B* **85**, 125304 (2012).
- [22] Oestreich, M., Römer, M., Haug, R. J. & Hägele, D. Spin Noise Spectroscopy in GaAs. *Phys. Rev. Lett.* **95**, 216603 (2005).
- [23] Crooker, S. A., Cheng, L. & Smith, D. L. Spin noise of conduction electrons in n-type bulk GaAs. *Phys. Rev. B* **79**, 035208 (2009).
- [24] Römer, M. *et al.* Electron-spin relaxation in bulk GaAs for doping densities close to the metal-to-insulator transition. *Phys. Rev. B* **81**, 075216 (2010).
- [25] Heisterkamp, F. *et al.* Longitudinal and transverse spin dynamics of donor-bound electrons in fluorine-doped ZnSe: Spin inertia versus Hanle effect. *Phys. Rev. B* **91**, 235432 (2015).
- [26] Belykh, V. V. *et al.* Extended pump-probe Faraday rotation spectroscopy of the submicrosecond electron spin dynamics in n-type GaAs. *Phys. Rev. B* **94**, 241202 (2016).
- [27] Altshuler, B. L. & Aronov, A. G. *Electron-Electron Interactions in Disordered Systems* (Elsevier, Amsterdam, 1985).
- [28] Fritzsche, H. & Lark-Horovitz, K. Electrical Properties of p-Type Indium Antimonide at Low Temperatures. *Phys. Rev.* **99**, 400–405 (1955).
- [29] Woods, J. F. & Chen, C. Y. Negative Magnetoresistance in Impurity Conduction. *Phys. Rev.* **135**, A1462–A1466 (1964).
- [30] Halbo, L. & Sladek, R. J. Magnetoresistance of Undoped n-Type Gallium Arsenide at Low Temperatures. *Phys. Rev.* **173**, 794–802 (1968).
- [31] Benzaquen, M., Walsh, D. & Mazuruk, K. Low-field magnetoresistance of n-type GaAs in the variable-range hopping regime. *Phys. Rev. B* **38**, 10933–10936 (1988).

- [32] Kawabata, A. Theory of negative magnetoresistance in three-dimensional systems. *Solid State Commun.* **34**, 431–432 (1980).
- [33] Kawabata, A. Theory of Negative Magnetoresistance I. Application to Heavily Doped Semiconductors. *J. Phys. Soc. Japan* **49**, 628–637 (1980).
- [34] Capoen, B., Biskupski, G. & Briggs, A. Low-temperature conductivity and weak-localization effect in barely metallic GaAs. *J. Phys. Condens. Matter* **5**, 2545–2552 (1993).
- [35] Lyubinskiy, I. S. & Kachorovskii, V. Y. Hanle Effect Driven by Weak Localization. *Phys. Rev. Lett.* **94**, 076406 (2005).
- [36] Ivchenko, E. L. Spin relaxation of free carriers in semiconductors without inversion center in longitudinal magnetic field. *Fiz. Tverd. Tela* **15**, 1566 (1973) [Sov. Phys. Solid State 15, 1048 (1973)].
- [37] Glazov, M. M. & Ivchenko, E. L. Precession spin relaxation mechanism caused by frequent electron-electron collisions. *JETP Lett.* **75**, 403–405 (2002).
- [38] Glazov, M. M. & Ivchenko, E. L. Effect of electron-electron interaction on spin relaxation of charge carriers in semiconductors. *J. Exp. Theor. Phys.* **99**, 1279–1290 (2004).
- [39] Jusserand, B., Richards, D., Allan, G., Priester, C. & Etienne, B. Spin orientation at semiconductor heterointerfaces. *Phys. Rev. B* **51**, 4707–4710 (1995).
- [40] Richards, D. & Jusserand, B. Spin energetics in a GaAs quantum well: Asymmetric spin-flip Raman scattering. *Phys. Rev. B* **59**, R2506–R2509 (1999).
- [41] Bronold, F. X., Martin, I., Saxena, A. & Smith, D. L. Magnetic-field dependence of electron spin relaxation in n-type semiconductors. *Phys. Rev. B* **66**, 233206 (2002).
- [42] Gor'kov, L. P., Larkin, A. I. & Khmel'nitski, D. E. Particle conductivity in a two-dimensional random potential. *JETP Lett.* **30**, 228 (1979).
- [43] Dmitriev, A. P., Kachorovskii, V. Y. & Gornyi, I. V. Non-backscattering contribution to weak localization. *Phys. Rev. B* **56**, 9910–9917 (1997).
- [44] Isawa, Y. Inelastic Scattering Time in Disordered Metals. *J. Phys. Soc. Japan* **53**, 2865–2867 (1984).